

## Superfluid helium in fully saturated porous media

Kerson Huang

*Department of Physics and Center for Theoretical Physics, Laboratory for Nuclear Science,  
Massachusetts Institute of Technology, Cambridge, Massachusetts 02139*

Hsin-Fei Meng

*Department of Mathematics, Massachusetts Institute of Technology, Cambridge, Massachusetts 02139*

(Received 8 April 1993)

The flow of superfluid  $^4\text{He}$  through spongelike media at full saturation is modeled by the flow of current through an Ohmic network with random resistors. Solving Kirchhoff's equations leads to the conclusion that the superfluid critical point is a percolation threshold, with critical exponent 1.7. The fractal dimension of the percolating cluster is 2.6. These lead to a specific-heat exponent  $\alpha = -5.4$ , by the Josephson hyperscaling relation. Existing experiments apparently do not cover the critical region. Instead, they measure "mean-field" exponents, whose values for Vycor, aerogel, and xerogel can all be reproduced by choosing appropriate distribution functions for the resistors.

There have been many experimental studies of superfluid  $^4\text{He}$  adsorbed in the spongelike media Vycor, aerogel, and xerogel, with porosities ranging from 30 to 96%.<sup>1-4</sup> The superfluid density and specific heat have been measured, for wide ranges of coverage, from a few atomic layers to full saturation, and for wide ranges of temperature below the  $\lambda$  point of bulk liquid helium. The superfluid transition temperature is found to decrease with decreasing coverage, extrapolating to zero at a nonzero critical coverage. Thus, superfluidity disappears below a critical coverage, even at absolute zero. Near the critical coverage, the superfluid exponent has the ideal-gas value  $\zeta = 1$ . When the coverage is increased from the critical value, however, different physics takes over at some point, for  $\zeta$  is observed to cross over to a different value. At full saturation, the  $\zeta$  for Vycor, and xerogel are respectively 0.67 and 0.89.<sup>2</sup> For aerogel, the values are 0.80 according to Ref. 2, and 0.75 according to Ref. 4. For comparison,  $\zeta = 0.672$  for the bulk liquid. In an earlier work,<sup>5</sup> we demonstrated the disappearance of superfluidity at absolute zero in a dilute hard-sphere Bose gas in random potentials, due to boson localization, i.e., pinning of the Bose condensate by the random potentials. In this paper, we consider the full-saturation case, and propose a model that can explain some of the observations in that regime.

We model the flow channels in the spongelike medium as bonds in a cubic lattice, with channel radii chosen at random from a given distribution. We have considered two types of distributions: a Gaussian distribution with adjustable center and width, and a uniform distribution with adjustable lower and upper cutoffs. In either case, the medium is characterized by two parameters.

In a long channel of radius  $r$  filled with liquid  $^4\text{He}$ , the superfluid transition temperature  $T_c(r)$  decreases with  $r$ , for large  $r$ , according to a power law:<sup>6</sup>

$$1 - T_c(r)/T_\infty \approx (r/r_0)^{-q}, \quad (1)$$

where  $q \approx 2$ ,  $r_0 \approx 5$  nm, and  $T_\infty = 2.172$  K is the bulk

transition temperature. We use a simple interpolation formula for all  $r$ :  $T_c(r)/T_\infty = 1 - [1 + (r/r_0)^q]^{-1}$ . The superfluid density in a channel of radius  $r$  at temperature  $T$ , denoted by  $\rho_s(r, T)$ , is of course zero for temperatures  $T > T_c(r)$ . For  $0.9 < [T/T_c(r)] < 1$ , we take

$$\rho_s(r, T) = K_1 [1 - T/T_c(r)]^\xi, \quad (2)$$

where  $\xi = 0.67$  is the bulk critical exponent and  $K_1$  a constant. Outside of the indicated interval we use a polynomial form that reduces to  $1 - K_2 T^2$  near  $T = 0$ , and joins smoothly to the formula above. Our results are not sensitive to how we interpolate. The channel lengths are effectively infinite. How realistic this assumption is will be discussed later.

The momentum density for superfluid flow is given by  $\mathbf{j} = \rho_s \mathbf{v}_s + \rho_n \mathbf{v}_n$ , where the two terms refer to the superfluid and normal fluid, respectively. Assuming that all channels are so small that the normal fluid is pinned, we put  $\mathbf{v}_n = 0$ . Thus, writing  $\mathbf{v}_s = \nabla \phi$ , where  $\phi$  is proportional to the superfluid phase, we have

$$\mathbf{j} = \rho_s \nabla \phi. \quad (3)$$

This looks like Ohm's law with current density  $\mathbf{j}$ , electrostatic potential  $\phi$ , and electrical conductivity  $\rho_s$ . Thus, each bond can be replaced by a resistor, and the superfluid density of the medium corresponds to the conductivity of the network. Because of the close analogy, we shall freely use the language of the electrical analog when convenient.

After assigning the bond radii, and with that the electrical resistances, we calculate the conductivity of the network by solving Kirchhoff's equations numerically, using Gauss-Seidel iteration with (simultaneous overrelaxation) SOR.<sup>7</sup> We use lattice sizes  $10^3$  and  $20^3$ , with some calculations done on  $30^3$  and  $50^3$  lattices. In the following, we summarize the insight gained from the computer simulations, illustrated with plots of quantitative results, and conclude with some critical remarks.

Imagine that a voltage (superfluid phase) difference is established between the top and bottom plates of the lattice, taken to be equipotentials. At high temperatures all channels are closed, and the network is nonconducting (no superfluid flow.) As the temperature is lowered, some channels become conducting, but the whole network remains nonconducting until a percolating cluster of open bonds connects the top to the bottom plate. The percolation threshold  $T_0$  (which is not the  $T_c$  of the experiments) is the true critical point for the onset of superfluidity. The behavior near this threshold, in a finite lattice, has a complicated structure. When the temperature is decreased, opening up a single bond can appreciably enlarge the percolating cluster. As a result, the superfluid density exhibits a series of bumps with discontinuous derivatives. The slope at the beginning of each bump corresponds approximately to the bulk critical exponent  $\xi$ , which is an input to the calculation. This behavior is illustrated in Fig. 1(a), where the cluster size, as well as the fraction of open channels, are also shown. When we go to a larger lattice, the bumps in the superfluid density tend to be smoothed out. The critical exponent  $\xi_0$  for an infinite lattice can be approximately calculated by averaging over these bumps. We obtain in this fashion  $\xi_0 \approx 1.7$ , which agrees with numerical results

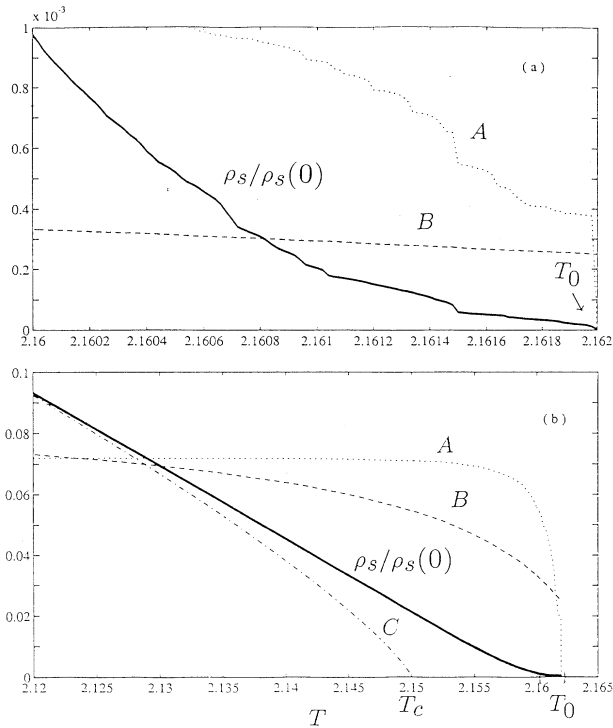


FIG. 1. Panel (a) shows the superfluid density from the computer simulation as a function of temperature, very near the percolation threshold. Curve *A* shows the percolating cluster size, and curve *B* shows the fraction of open bonds. Lattice size is  $20^3$ , with a Gaussian distribution of bond radii. Panel (a) is an enlargement from (b), whose temperature range is shown in (b) enclosed in curly brackets. The very beginning of the mean-field region now comes into view. Curve *C* is the power-law fit that determines  $\xi$  and  $T_c$ .

on percolation in 3D.<sup>8</sup>

The specific heat at percolation threshold behaves like

$$C = (A/\alpha)|T_0 - T|^{-\alpha} + B, \quad (4)$$

where  $A$  and  $B$  are constants. Josephson hyperscaling<sup>9</sup> predicts  $\xi_0 d = (2 - \alpha)(d - 2)$ . Using  $\xi_0 = 1.7$  and  $d = d_f = 2.6$ , we obtain for the specific-heat exponent  $\alpha = -5.4$ , which would make it difficult to detect the singularity experimentally. Specific-heat peaks were observed in aerogel at full saturation in Ref. 3, which also reports slight shifts of  $T_0$  in different samples of aerogel cut from the same block. The latter can be explained by the dependence of the percolation threshold on pore distribution. The peaks observed in Ref. 3 are probably due to crossover to a “mean-field” region discussed below, the true critical region being buried in the sharp rise of the specific heat.

When the temperature is decreased from the percolation region, the system crosses over to a mean-field regime, in which the superfluid density has a different power-law behavior, with exponent  $\xi$ . This is shown in Fig. 1(b) and the process is continued in Fig. 2. The mean-field region corresponds to that studied extensively in experiments, while the crossover region corresponds to the “tails” in the data that have always been ignored.

The difference between the mean-field and the critical regions is revealed by measuring the fractal dimension  $d_f$  of the percolating cluster in the computer. As shown in Fig. 3,  $d_f \approx 2.6$  at the percolating threshold, which agrees with previous numerical results.<sup>10</sup> With decreasing tem-

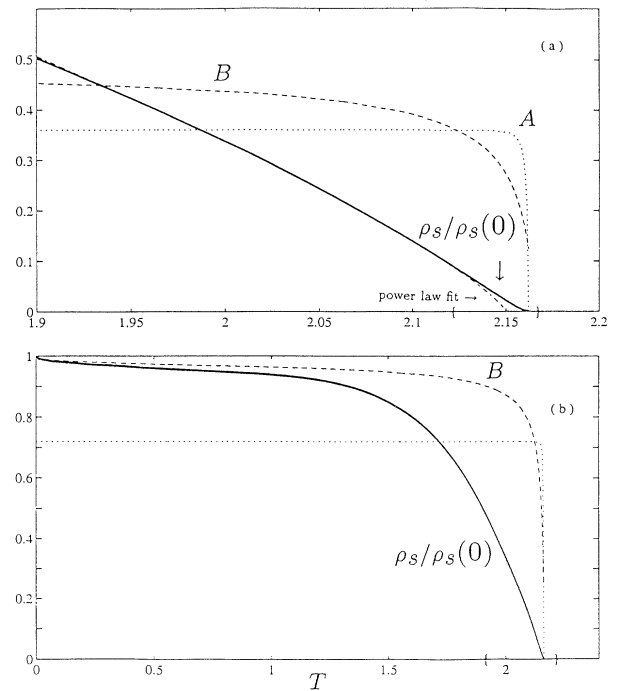


FIG. 2. Panels (a) and (b) continue from Fig. 1(b). The temperature interval covered in the previous region is enclosed in curly brackets. In (a) the mean-field region is fully visible, together with the power-law fit. In (b) the power-law fit becomes indistinct.

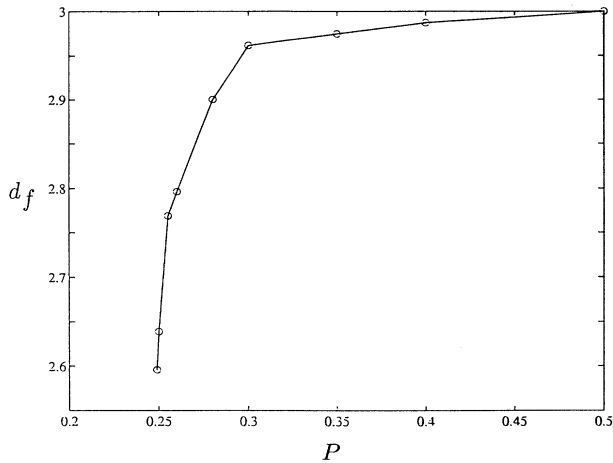


FIG. 3. Fractal dimension  $d_f$  of the percolating cluster as a function of the fraction of open bonds  $p$ . The latter was given as a function of temperature in curve  $B$  of Fig. 1(a). The simulation was done in a  $50^3$  lattice.

perature,  $d_f$  rapidly rises toward 3, when the mean-field region is established. Almost all sites are then connected to the percolating cluster (though not necessarily all bonds are open.) In the mean-field region, a continuum approximation gives

$$\rho_s(T) = \int_0^\infty dr P(r) \rho_s(r, T), \quad (5)$$

where  $P(r)dr$  is the probability that the radius of a channel lies between  $r$  and  $(r + dr)$ .

We determine  $\zeta$  by introducing an effective transition temperature  $T_c$ , plotting the computed superfluid density against  $T_c - T$  in a log-log plot, and adjusting  $T_c$  until a straight line obtains for a range deemed significant. The method involves subjective judgment, but it is precisely that used on the experimental data.<sup>11</sup> Since  $\zeta$  is not associated with critical phenomena, there is no reason to expect it to have universality. It depends strongly on the distribution function of the radii. The discrepancy in the aerogel results between Refs. 2 and 4 might be due to differences in distribution functions. In Fig. 4(a), we plot  $\zeta$  for a Gaussian distribution as a function of the width of the distribution. Figure 4(b) shows that for a uniform distribution, as a function of the upper cutoff. The observed values for Vycor, aerogel, and xerogel can all be reproduced.

Examples of the log-log plots used to determine  $\zeta$  are shown in Fig. 5, where we include three choices of the distribution function that can reproduce the experimental data for Vycor, aerogel, and xerogel, respectively. In the following, we comment on the comparison with experimental data.

Vycor is known to have relatively uniform pore radii, which are small compared to channel lengths.<sup>1,12</sup> The assumptions in our model are tailored for this case, and we can fit both  $\zeta$  and the crossover region rather well. It is not surprising that  $\zeta$  lies close to the bulk value, while  $T_c$  does not. In the extreme case where all pores sizes are exactly the same, the percolation cluster would be sa-

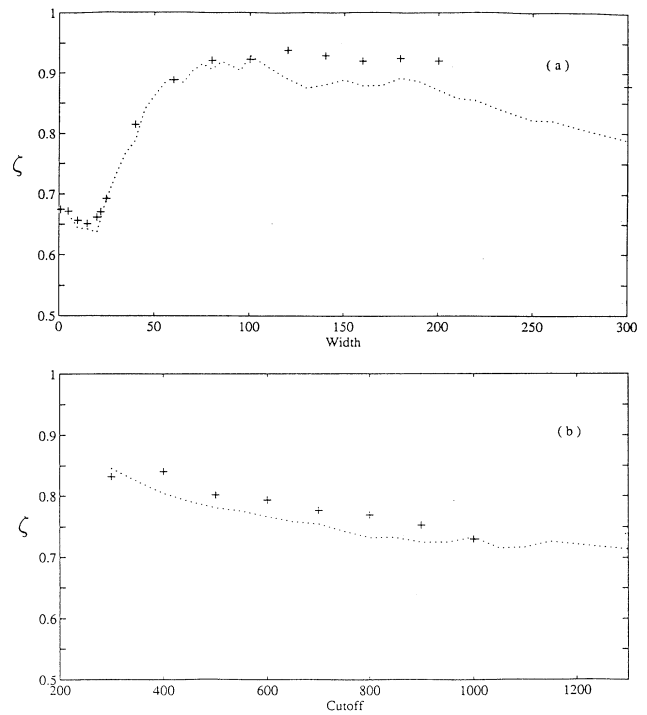


FIG. 4. The effective exponent  $\zeta$  as a function of parameters that define the disordered medium. The crosses are from computer simulations, and the curves are obtained using the continuum approximations [Eq. (5)]. In (a) the radius distribution is a Gaussian centered at  $100 \text{ \AA}$ , with variable width in angstroms. In (b) the distribution is uniform from zero to a variable upper cutoff in angstroms.

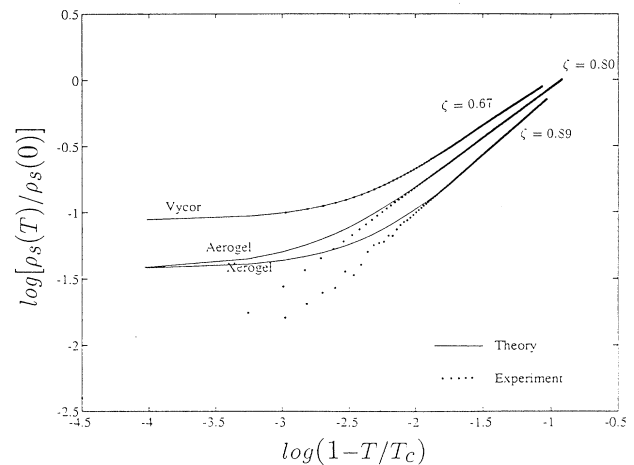


FIG. 5. Log-log plot of superfluid density against  $T_c - T$ , where  $T_c$  has been adjusted to yield the best straight line in the mean-field region. The distribution functions are chosen to reproduce  $\zeta$ . The curves have been displaced vertically relative to one another, for visual comparison of the slopes. The dots are experimental points read off the graphs in Ref. 2.

turated as soon as it occurs, and  $\zeta$  would have the input bulk value. The transition temperature, however, would be depressed by the finite pore size.

Aerogel has fractal structure, and the pores are not particularly channel-like.<sup>13</sup> Our best chance is to choose a broad distribution of radii. Not surprisingly, this makes  $\zeta$  different from the bulk value, but brings  $T_c$  closer to bulk value, because of the prevalence of large pores. Although  $\zeta$  can be fit by adjusting the width of the distribution, the data show a wide mean-field region.

Xerogel is essentially collapsed aerogel, and has long channels along which the radius varies, because small offshooting branches have been pinched shut.<sup>14</sup> Again, we can fit  $\zeta$  but not to the extent of the mean-field region. A better model for this case might be to allow the channel to have segments of varying radii.

We feel confident that the fits for the aerogel and xerogel data can be fit, essentially perfectly, by introducing more adjustable parameters. Our main purpose, however, is not to produce good fits, but to point out that existing experiments may have missed the true critical regions, which should be governed by a universal critical exponent of 1.7. To show that this is not ruled out by present data, we show in Fig. 6 a log-log plot of the low-temperature tails in existing data, which have been excluded in fits for the mean-field exponent. The "true" critical temperature  $T_c$  is adjusted for each medium so as to obtain the best straight line.

Further studies are needed to clarify the nature of the critical point, particularly concerning finite-size scaling, and effects of thermal fluctuations.

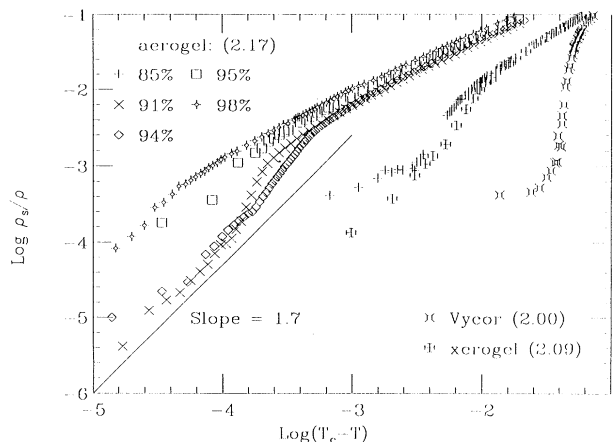


FIG. 6. Log-log plot of superfluid density against  $T_c - T$ , where values for  $T_c$ , the true critical temperature, are given in parentheses. They are adjusted to give the best straight line in the critical region. The data do not rule out a universal critical exponent of 1.7. We obtained the 85, 95, and 98 % aerogel data through the courtesy of M. W. H. Chan and J. Ma, and the 91 and 94 % aerogel data, and the xerogel and Vycor data, through the courtesy of J. Reppy and P. Crowell.

We thank Mehran Kardar for discussions. For making available experimental data we thank Moses Chan, Paul Crowell, Jian Ma, and John Reppy. This work is supported in part by funds provided by the U. S. Department of Energy under Contract No. DE-AC02-76ER03069.

<sup>1</sup>For a comprehensive review, see J. D. Reppy, *J. Low Temp. Phys.* **87**, 205 (1992).

<sup>2</sup>M. H. W. Chan, K. I. Blum, S. Q. Murphy, G. K. S. Wong, and J. D. Reppy, *Phys. Rev. Lett.* **61**, 1950 (1988).

<sup>3</sup>G. K. S. Wong, P. A. Crowell, H. A. Cho, and J. D. Reppy, *Phys. Rev. Lett.* **65**, 2410 (1990).

<sup>4</sup>N. Mulders, R. Mehrotra, L. Goldner, and G. Ahlers, *Phys. Rev. Lett.* **67**, 695 (1991).

<sup>5</sup>K. Huang and H. F. Meng, *Phys. Rev. Lett.* **69**, 644 (1992).

<sup>6</sup>R. Donnelly, R. Hills, and P. Roberts, *Phys. Rev. Lett.* **42**, 75 (1979).

<sup>7</sup>W. H. Press, B. P. Flannery, S. A. Teukolsky, and W. T.

Vetterling, *Numerical Recipes* (Cambridge University Press, Cambridge, England, 1986), Sec. 17.5.

<sup>8</sup>J. Straley, *Phys. Rev. B* **15**, 5733 (1977).

<sup>9</sup>B. Josephson, *Phys. Lett.* **21**, 608 (1966).

<sup>10</sup>D. Stauffer and A. Aharony, *Introduction to Percolation Theory*, 2nd ed. (Taylor & Francis, London, 1992), p. 10.

<sup>11</sup>G. K. S. Wong, Ph.D. thesis, Cornell University, 1990.

<sup>12</sup>K. I. Blum, Ph.D. thesis, Cornell University, 1989.

<sup>13</sup>*Aerogels: Proceedings of the First International Symposium*, edited by J. Fricke (Springer-Verlag, Berlin, 1988).

<sup>14</sup>M. W. Shafer, D. D. Awshalom, J. Warnock, and G. Ruben, *J. Appl. Phys.* **C1**, 5438 (1987).